Original Article
LncRNA TEX41 regulates autophagy by increasing Runx2 expression in lung adenocarcinoma bone metastasis

Rong Li[1*], Yanping Lin[1*], Fengdi Hu[1], Yedan Liao[1], Jiadai Tang[1], Yan Shen[1], Heng Li[2], Jiangyan Guo[3], Lin Xie[1]

[1]Department of Gastrointestinal Oncology, The Third Affiliated Hospital of Kunming Medical University, Yunnan Cancer Hospital, Yunnan Cancer Center, Kunming, Yunnan, China; [2]2nd Department of Thoracic Surgery, The Third Affiliated Hospital of Kunming Medical University, Yunnan Cancer Hospital, Yunnan Cancer Center, Kunming, Yunnan, China; [3]Department of Pathology, The Third Affiliated Hospital of Kunming Medical University, Yunnan Cancer Hospital, Yunnan Cancer Center, Kunming, Yunnan, China. *Equal contributors.

Abstract: Objective: To investigate the mechanism underlying the role of TEX41 in lung adenocarcinoma (LUAD) bone metastasis (BM). Methods: We analyzed the biological functions and molecular mechanisms of TEX41 using bioinformatics. TEX41 and Runx2 expressions were measured in clinical tissue samples and cell lines by quantitative PCR. The effects of TEX41 on LUAD cell proliferation, migration, invasion and metastasis as well as its mechanism of action were investigated. Fluorescence in-situ hybridization (FISH) was performed to determine TEX41 and Runx2 colocalization. Subcutaneous tumor growth and BM were evaluated in nude mice by X-ray and hematoxylin and eosin (HE) staining. Results: TEX41 was dramatically increased in LUAD BM tissue, indicating a poorer prognosis in patients with LUAD and BM. TEX41 knockdown suppressed the migration and metastasis of LUAD cells, whereas TEX41 overexpression promoted these processes. Data from X-ray and HE staining showed that TEX41 supported the BM in LUAD. TEX41 overexpression induced autophagy in LUAD cells, as demonstrated by changes in autophagy markers. Results of FISH showed that TEX41 and Runx2 colocalized in the nucleus, and Runx2 expression was regulated by TEX41. The effects of TEX41 on LUAD cell migration, invasion, metastasis and autophagy were counteracted by Runx2 inhibition. Moreover, the role of TEX41 in the metastasis was partially dependent on autophagy, and phosphoinositide 3-kinase (PI3K)-AKT might be the major signaling pathway involved in TEX41-regulated autophagy. Conclusion: TEX41 promotes autophagy in LUAD cells by upregulating Runx2 to mediate LUAD migration, invasion and BM.

Keywords: LncRNA TEX41, Runx2, LUAD, bone metastasis, autophagy

Introduction

Lung cancer has the second highest incidence (11.4%) and the highest mortality (18%) among cancers, with approximately 1.8 million deaths worldwide in 2020 [1]. Lung adenocarcinoma (LUAD) has become the leading type of histological lung cancers, accounting for 50% of lung cancer cases today [2]. Although rapid progress has been made in identifying treatments for LUAD, the 5-year survival rate for advanced LUAD is only 2-5% [3, 4]. LUAD is prone to distant metastasis, especially bone metastasis (BM), with 30-40% of patients developing BM at advanced disease stages [5].

The median survival time after diagnosis of BM in LUAD is approximately 1 year [6]. Therefore, a better understanding of the pathogenic mechanisms underlying BM in LUAD is critical for finding novel treatments.

The most common noncoding RNAs are long noncoding RNAs (lncRNAs), which are longer than 200 bp and account for more than 80% of all RNAs [7]. LncRNAs play diverse and complex roles in various regulatory processes, including development, differentiation, metabolism, genomic imprinting and transcriptional regulation [8]. Abnormal lncRNA expression is tightly linked to tumorigenesis, progression,

recurrence, metastasis and chemotherapy resistance [9-11]. Thus, lncRNAs could aid in diagnosing disease and determining prognosis and can be novel therapeutic targets. Several lncRNAs (e.g., MALAT-1 [12], HOTAIR [13], CCAT2 [14], GSEC [15], MAFG-AS1 [16], NEAT1 [17], PCAT19 [18] and HITT [19]) are involved in the progression of non-small cell lung cancers. Autophagy is a solid tumor survival mechanism, but its roles in the inhibition or promotion of tumor development remain controversial [20-23]. Several LncRNAs (e.g., lncRNA RP11-295G20.2, NFYC-AS1 and FIRRE) can regulate autophagy to affect tumor cell migration and invasion [24-28].

We previously investigated differentially expressed genes in LUAD BM by transcriptomic sequencing and bioinformatics analyses of LUAD and BM tissue samples [29]. In the current study, we examined TEX41, a newly discovered lncRNA that has recently been associated with some tumors, although the specific mechanism of TEX41 action in LUAD has not yet been reported. We found that TEX41 could affect LUAD progression by regulating autophagy via Runx2. Thus, the TEX41-Runx2-autophagy signaling pathway could be a potential target for the treatment of BM in LUAD.

Materials and methods

Bioinformatic analysis of TEX41

Gene Ontology (GO) functional annotation and Kyoto Encyclopedia of Genes and Genomes (KEGG) pathway enrichment analysis were performed for differentially expressed TEX41 target genes. The cellular localization of TEX41 was analyzed with lncATLAS. Transcription factors associated with TEX41 target genes were predicted using the TFBSTools R package.

Patients and samples

This study included 28 surgical LUAD cases without distant metastases who underwent curative resection and 20 LUAD cases with BM who underwent palliative surgery in Yunnan Cancer Hospital between January and December 2019. The resected primary LUAD lesion, adjacent paracancerous tissue and excised BM tissue were collected. The study was approved by the Medical Ethics Committee of Yunnan Cancer Hospital. The patients provided written informed consent.

Inclusion criteria for LUAD without metastasis included patients who were at first diagnosis of LUAD, without preoperative antitumor treatment (e.g., radiotherapy or chemotherapy), with tumor stages I-III, and with complete clinico-pathological data. Inclusion criteria for LUAD with BM included patients with LUAD diagnosed with BM by palliative surgery and with complete clinicopathological data. Patients were excluded for both groups if they had other malignant tumors or serious psychiatric diseases.

Tissue samples were immediately immersed in cryovials containing approximately 1 ml RNAlater solution (Sigma, USA) after collection. The cryovials were placed in a 4°C freezer within 30 min and transferred to a liquid nitrogen tank after overnight.

Quantitative polymerase chain reaction (qPCR)

RNA was isolated using TriQuick Reagent (Solarbio, Beijing, China). Reverse transcription was performed using the Takara Primescript RT Reagent Kits with gDNA eraser (Takara Bio, Shiga, Japan). qPCR was performed using SYBR Green Mastermix (Takara Bio) with a 7500 Fast Dx Real-Time PCR Instrument (ABI, USA). The qPCR conditions consisted of 95°C for 15 min followed by 40 cycles of 95°C for 10 s and 66°C for 32 s. RNA expression data were normalized to the expression level of the control gene glyceraldehyde-3-phosphate dehydrogenase (GAPDH). The qPCR primers (5'-3') were: TEX41 forward: TCCC-TTCGAGTAACACCCACA, TEX41 reverse: GAT-TTTCCCCTGGGTCTCACA; Runx2 forward: TG-GTTACTGTCATGGCGGGTA, Runx2 reverse: TC-TCAGATCGTTGAACCTTGCTA; GAPDH forward: CTGGGCTACACTGAGCACC, GAPDH reverse: AAGTGGTCGTTGAGGGCAATG. Fold change was calculated using the $2^{-\Delta\Delta Ct}$ method.

Cell culture and transfection

Human LUAD cells (A549, H838, H1734 and H1299) and normal bronchial epithelial cells (Beas-2B) were obtained from the Kunming Institute of Zoology. A549, H838 and H1734 cells were cultured in RPMI-1640 with 10% fetal bovine serum (FBS, Gibco, Grand Island, NY) and 1% penicillin/streptomycin (Hyclone, Logan, Utah, USA). H1299 and Beas-2B cells were maintained in DMEM (Gibco, Grand Island, NY) containing 10% FBS and 1% penicillin/streptomycin. All cells grew in a 37°C incubator

with 5% CO_2. TEX41 interference (sh-TEX41) and overexpression (OE-TEX41) lentivirus vectors and the corresponding negative control (NC) vectors (sh-NC and OE-NC) were generated by OBIO Co., LTD (Shanghai, China). Three small hairpin RNA (shRNA) fragments targeting TEX41 were inserted into a pSLenti-U6-shRNA (TEX41)-CMV-EGFP-F2A-Puro-WPRE individually (sh-TEX41-1: 5'-GGGCAAGCCACAG-AAACAA-3', sh-TEX41-2: 5'-GCAGGGAGAAGTG-TTGCTT-3', and sh-TEX41-3: 5'-CCTACCATAGT-TTACCTAA-3'), and a negative control shRNA (sh-NC, 5'-CCTAAGGTTAAGTCGCCCTCG-3) was used. sh-TEX41-1 was used for subsequent experiments because of its high interference efficiency and stability. TEX41 (full-length cDNA) was inserted into a GL151 pASLenti-pA-MCS-CMV-EF1-EGFP-WPRE vector to construct the TEX41 overexpression vector. The lentivirus was transduced into H838 or A549 cells to construct stable cell lines. For Runx2 and autophagy experiments, cells were treated with the Runx2 protein inhibitor CADD522 (10 µM) or the autophagy inducer rapamycin (1 µM) for 48 h.

Cell Counting Kit-8 (CCK-8) and colony-forming assays

For the CCK-8 assay, LUAD cells were seeded in 96-well plates (3 × 10³/well, five replicate wells per group) and cultured at 37°C. To measure proliferation, CCK-8 test reagent (10 µl; Dojindo, Kumamoto, Japan) was added to the cells at 0, 24, 48 or 72 h, and the optical density at 450 nm was measured with a Bio-Rad reader (Bio-Rad, Hercules, CA, USA).

For the colony-forming assay, LUAD cells (0.8 × 10³ cells/well) were seeded in 6-well plates and grew for 14 d. The experiment ended when macroscopic colonies were visible at the bottom of the wells. The cells were fixed with 4% paraformaldehyde (PFA) for 15 min and stained with 1% crystal violet for an additional 15 min. Colonies were photographed with a Leica camera and analyzed with ImageJ.

Wound healing assay

Cells (3 × 10⁵/well) were seeded into 6-well plates and grew to 80-90% confluency. Parallel lines were scratched in the monolayer with pipette tips, and the cells were maintained in serum-free medium. Wound healing was moni-

tored with an inverted microscope at 0, 12, 24 and 48 h. Cell migration was determined by the percentage change in the wound width. The results were analyzed with ImageJ.

In vitro invasion analysis

Invasion was assessed using the Transwell chambers (Corning, New York, USA). Diluted substrate gel (Sigma, USA) (100 µl) was added to the upper chamber, and cells (1 × 10⁴ cells/ml, 100 µl) were seeded in the upper chamber. The lower chamber was added with 500 µl medium containing 10% FBS. The cells were incubated for 24 h. Invading cells were fixed with 4% PFA for 15 min and then stained for 15 min with 1% crystal violet. Five randomly selected fields were counted using a microscope to determine the number of invasive cells.

Western blot

Proteins were isolated with radioimmunoprecipitation assay buffer (Beyotime, Shanghai, China) and quantified using the bicinchoninic acid kits (Beyotime). After sodium dodecyl-sulfate-polyacrylamide gel electrophoresis, proteins were transferred to polyvinylidene fluoride membranes (Millipore, Massachusetts, USA). The membranes were blocked with 5% non-fat milk in TBS-Tween (TBST) for 1 h and then incubated with primary antibodies (1:1000, Cell Signaling Technology, Danvers, MA, USA) at 4°C for 1-2 h. After four washes with TBST (10 min each), the membranes were incubated with horseradish peroxidase-labeled secondary antibody (1:1000) for 2 h. Staining was detected using ECL Western blotting kits (Biosharp, Shanghai, China). β-actin was used as an internal control.

In vivo proliferation and BM assays

Male BALB/c nude mice (4-5 weeks old) were obtained from Beijing Vital River Ltd., China, and maintained in a specific pathogen-free facility. The protocol was approved by the Institutional Animal Care and Use Committee of the Kunming Medical University Animal Center. The experiments involving animals followed the institutional guidance for the care and use of laboratory animals.

After feeding for one week, the mice were divided into four groups (sh-NC, sh-TEX41, OE-NC and OE-TEX41, n=4 per group). Tumor cells (1 ×

10^6/ml) were inoculated subcutaneously (200 µl) into the right axilla and bilaterally into the tibial cavities (100 µl). The mice were weighed every 5 d, and the subcutaneous tumors were measured in two dimensions (the longest dimension and the dimension perpendicular to the longest dimension) using calipers. After 35 d of tumor cell inoculation, X-rays were taken to evaluate tibial BM and bone destruction. Following euthanasia via cervical dislocation, subcutaneous tumor and BM tissue were collected, weighed and subjected to HE staining and immunoblotting.

Statistical analysis

Statistical analysis was performed with GraphPad Prism 8.0 (GRAPH PAD Software Inc., CA, USA). Measurement data for continuous variables were presented as mean ± standard deviation, and t-test, ANOVA followed by LSD test and repeated measures ANOVA were used for analyses of the continuous variables. Categorical variables were expressed as a percentage and compared by the Chi-square test. Survival curves were constructed using the Kaplan-Meier method and evaluated by the log-rank test. $P < 0.05$ was defined as significant.

Results

Bioinformatic analysis of TEX41

GO functional enrichment analysis was performed to identify potential TEX41 targets. Functional annotation of biological processes, molecular functions and cellular components showed that many TEX41 target genes were enriched in functions such as protein regulation, cell surface signaling pathways and tissue morphogenesis (**Figure 1A** and **1B**). KEGG analysis showed that TEX41 target genes were enriched in various tumor-related pathways, including the phosphoinositide-3-kinase (PI3K)-AKT pathway (**Figure 1C**). The PI3K-KT pathway is regulated by autophagy, which plays an important role in tumorigenesis [21]. Therefore, we focused on the cellular autophagy pathway. Enrichment analysis of TEX41 target genes in this pathway revealed that some TEX41 target genes were enriched in the autophagic pathway (**Figure 1D**).

The mechanisms of lncRNA actions are tightly linked to their cellular localizations. LncRNAs in the nucleus can epigenetically or transcription-

ally modulate gene expression by binding to chromatin modification complexes, shearing factors or transcription factors. Analysis of the lncATLAS database revealed that TEX41 largely resided in the nucleus (**Figure 1E**). Transcription factor and binding site prediction analysis indicated that Runx2 could be a transcription factor interacting on TEX41 (**Figure 1F**).

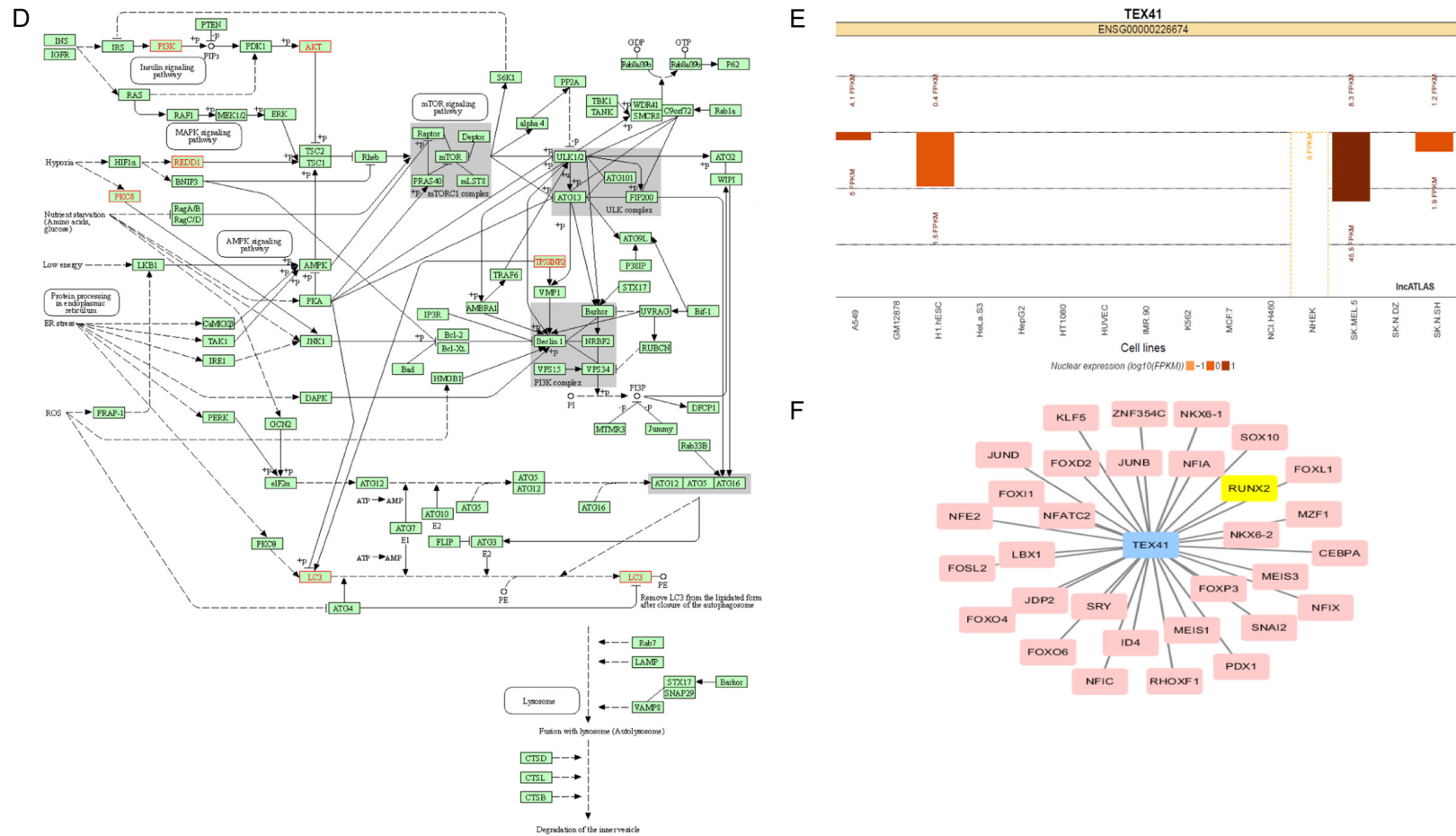*Expression and clinical significance of TEX41 in LUAD with BM*

TEX41 levels were measured in tumors and paired paracancerous tissue from 28 patients with non-metastatic LUAD. We found that TEX41 was highly expressed in primary LUADs compared with that in paired paracancerous tissue (**Figure 2A**). TEX41 levels were also assessed in tissues from 20 LUAD cases with BM, which indicated that TEX41 was drastically increased in LUAD BM compared with that in primary LUADs (**Figure 2B**). However, no differences in TEX41 levels were observed among LUADs in different sizes (**Figure 2C**). Higher TEX41 expression was associated with lymph node invasion and more advanced stages (**Table 1**; **Figure 2D** and **2E**). In LUAD patients with BM, higher TEX41 levels were associated with a worse prognosis (**Figure 2F**).

Silencing TEX41 inhibits the malignant biological behavior of LUAD cells

TEX41 levels were higher in LUAD cell lines (A549, H1734, H1299 and H838) than those in the normal bronchial epithelial cell line Beas-2B (**Figure 3A**). The expression of TEX41 was higher in H838 cells derived from LUAD lymph node metastases than that in A549 cells derived from a primary LUAD. To investigate the mechanism of TEX41 action, we generated a stable TEX41-knockdown H838 cell line using TEX41-targeting shRNA (**Figure 3B**) and a stable TEX41-overexpressing A549 cell line by introducing the full-length TEX41 coding region via a lentiviral construct (Figure S1A). Using the CCK-8 and colony-forming assays, we found that TEX41 knockdown inhibited the proliferation of H838 LUAD cells (**Figure 3C** and **3D**). Moreover, results of the wound healing assay and Transwell assay showed that TEX41 knockdown prevented H838 migration and invasion (**Figure 3E** and **3F**). We also examined the effects of TEX41 interference on key proteins involved in epithelial-mesenchymal transition (EMT) and found that TEX41 knockdown

A

B

ID	Description
GO:0007275	multicellular_organism_development
GO:0007165	signal_transduction
GO:0005886	plasma_membrane
GO:0005829	cytosol
GO:0031981	nuclear_lumen
GO:0048513	animal_organ_development
GO:0005654	nucleoplasm
GO:0051173	positive_regulation_of_nitrogen_compound_metabolic_proces
GO:0031325	positive_regulation_of_cellular_metabolic_process
GO:0019538	protein_metabolic_process

C

Figure 1. Bioinformatics analysis of TEX41. A, B. Gene Ontology enrichment analysis of differentially expressed TEX41 target genes. C. Kyoto Encyclopedia of Genes and Genomes enrichment analysis of differentially expressed TEX41 target genes. D. Accumulation analysis of TEX41 target genes in the autophagic pathway. E. TEX41 cell localization analysis using the LncATLAS database. F. Prediction of the TEX41-associated transcription factors.
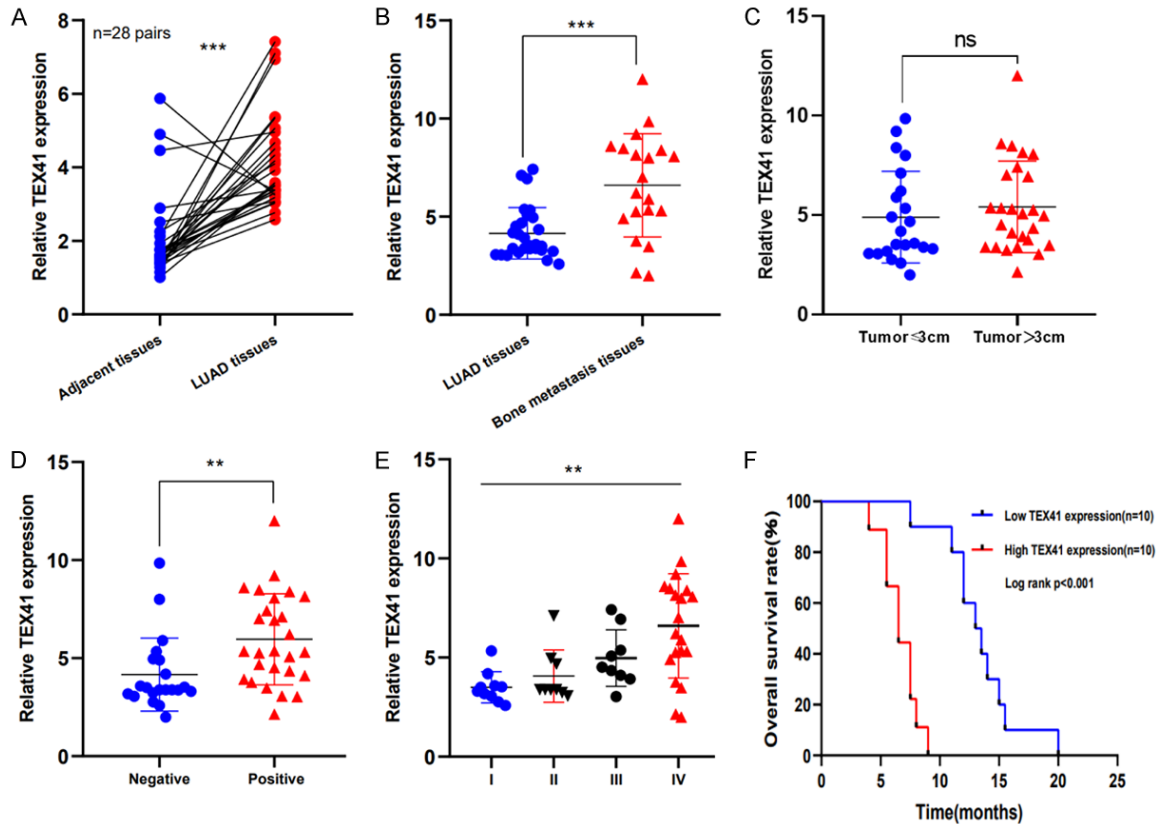
Figure 2. TEX41 was increased in lung adenocarcinoma (LUAD) with bone metastasis (BM) and correlated with prognosis. A. TEX41 expression in primary LUAD. B. TEX41 expression in LUAD BM. C-E. TEX41 expression in LUAD of different sizes, with and without lymph node metastases, and at different tumor stages. F. Kaplan-Meier curves for the effect of TEX41 levels on overall survival among 20 patients with LUAD and BM. The dataset median was used to determine "High TEX41" and "Low TEX41". *$P<0.05$, **$P<0.01$, ***$P<0.001$.

increased E-cadherin levels and suppressed vimentin (**Figure 3G**), suggesting that TEX41 knockdown could reduce LUAD cell metastasis. Conversely, the same cell function assays showed that TEX41 overexpression promoted the growth, migration and invasion of LUAD A549 cells (Figure S1B-F).

TEX41 affects the migration, invasion and metastasis of LUAD cells via Runx2

Our previous study and current bioinformatics analysis suggested that TEX41 and Runx2 might play important roles in LUAD BM [29]. Runx2 levels in clinical tissue samples were evaluated to further explore the underlying mechanism. We observed that Runx2 was highly expressed in primary LUAD tissue and even at a higher level in BM (**Figure 4A** and **4B**). Moreover, Runx2 was highly expressed in the LUAD cell lines A549, H1734, H1299 and H838 (**Figure 4C**). Immunoblotting showed that Runx2 protein levels were elevated in A549

and H838 cells, with H838 cells having a higher level (**Figure 4D**). TEX41 knockdown inhibited Runx2 expression, whereas TEX41 overexpression induced Runx2 expression (**Figure 4E-H**). FISH demonstrated that TEX41 and Runx2 colocalized in the nucleus (**Figure 4I**). Furthermore, treatment of TEX41-over-expressing A549 with CADD522, a specific inhibitor of Runx2-DNA binding, effectively counteracted the migratory, invasive and meta-static phenotypes mediated by TEX41 overexpression (**Figure 4J-L**), demonstrating that the oncogenic effects of TEX41 may be facilitated through Runx2.

TEX41 regulates the migration, invasion and metastasis of LUAD cells by mediating autophagy

Bioinformatics analysis suggested that TEX41 was linked to autophagy. To determine whether TEX41 regulates cellular autophagy in LUAD cells, we first examined changes in autophagy

Table 1. TEX41 levels and clinicopathological features

Characteristics	TEX41		P
	Low (n, %)	High (n, %)	
Sex			
Male	8 (32.0%)	17 (68.0%)	0.145
Female	13 (56.5%)	10 (43.5%)	
Age (years)			
≤60	16 (48.5%)	17 (51.5%)	0.366
>60	5 (33.3%)	10 (66.7%)	
Smoking history			
Yes	10 (35.7%)	18 (64.3%)	0.242
No	11 (55.0%)	9 (45.0%)	
Tumor stage			
I-III	17 (60.7%)	11 (39.3%)	0.008
IV	4 (20.0%)	16 (80.0%)	
Tumor size			
≤3 cm	11 (50.0%)	11 (50.0%)	0.561
>3 cm	10 (38.5%)	16 (61.5%)	
Lymphatic metastasis			
Yes	7 (25.9%)	20 (74.1%)	0.008
No	14 (66.7%)	7 (33.3%)	
Bone metastasis			
Yes	4 (20.0%)	16 (80.0%)	0.008
No	17 (60.7%)	11 (39.3%)	

marker proteins (p62, Beclin1 and LC3II/I) in stable TEX41 knockdown or overexpressing LUAD cells. We found increased p62 expression and decreased Beclin1 and LC3II/I expressions in H838 cells with TEX41 knockdown (**Figure 5A**). By contrast, increased Beclin1 and LC3II/I levels and decreased p62 level were observed in TEX41-overexpressing A549 cells (**Figure 5B**). It suggested that TEX41 is associated with autophagy in LUAD cells. Next, we examined the effects of TEX41 knockdown on autophagy in the presence of the autophagy inducer rapamycin, which reversed the inhibitory effects of TEX41 knockdown on cell migration, invasion and metastasis to some extent (**Figure 5C-E**), demonstrating that the oncogenic function of TEX41 might be partially dependent on autophagy. To further clarify whether TEX41 regulates autophagy through Runx2, we treated TEX41-overexpressing A549 cells with CADD522, a Runx2 inhibitor. CADD522 effectively counteracted the effects of TEX41 overexpression on autophagy (**Figure 5F**). However, the signaling pathway through which TEX41 regulates autophagy remains unclear. There-

fore, we examined the expression of key proteins involved in the classical autophagy pathway in TEX41-overexpressing A549 cells and found that phosphorylated (p)-PI3K, p-AKT and p-mechanistic targets of rapamycin were downregulated in response to TEX41 overexpression, whereas no significant changes were observed in the levels of p-AMP-activated protein kinase (**Figure 5G**). Therefore, TEX41 appears to regulate autophagy in LUAD cells via the PI3K-AKT signaling pathway.

TEX41 promotes the formation of subcutaneous LUAD tumors and BM in nude mice

We further elucidated the role and potential mechanism of TEX41 in LUAD with BM in nude mice. We injected H838 cells stably expressing sh-TEX41 or sh-NC, or A549 cells stably expressing TEX41 (OE-TEX41) or negative control (OE-NC) vectors into the right axilla and the bilateral tibia bones of nude mice. We found that mice in the sh-TEX41 group gained more weight than mice in the sh-NC group (**Figure 6A** and **6B**), whereas their subcutaneous tumors grew more slowly (**Figure 6C**). At the end of the study, the weights of the subcutaneous tumors and BM obtained from the sh-TEX41 group were lower than those from the sh-NC group (**Figure 6E** and **6G**). Moreover, HE staining suggested that the subcutaneous tumor differentiation of sh-TEX41 nude mice was better (**Figure 6D**). HE staining of tissue sections and X-rays of the nude mice indicated that the BM from the sh-TEX41 group showed lower levels of invasion and bone destruction than that from the control group (**Figure 6F** and **6H**). Furthermore, compared with that from the sh-NC group, the BM from the sh-TEX41 group showed no significant changes in Runx2 expression, but increased p62 levels and decreased Beclin-1 and LC3II/I levels were observed (**Figure 6I**). Compared with mice injected with OE-NC A549 cells, those with OE-TEX41 A549 cells experienced increased weight loss (Figure S2A and S2B), significantly increased subcutaneous tumor volumes (Figure S2C), more poorly differentiated (Figure S2D), increased weights for both subcutaneous tumors and BM (Figure S2E and S2G), and increased levels of BM invasion and bone destruction (Figure S2F and S2H). Compared with that from mice injected with OE-NC A549 cells, the BM from mice injected with OE-TEX41 A549 cells displayed
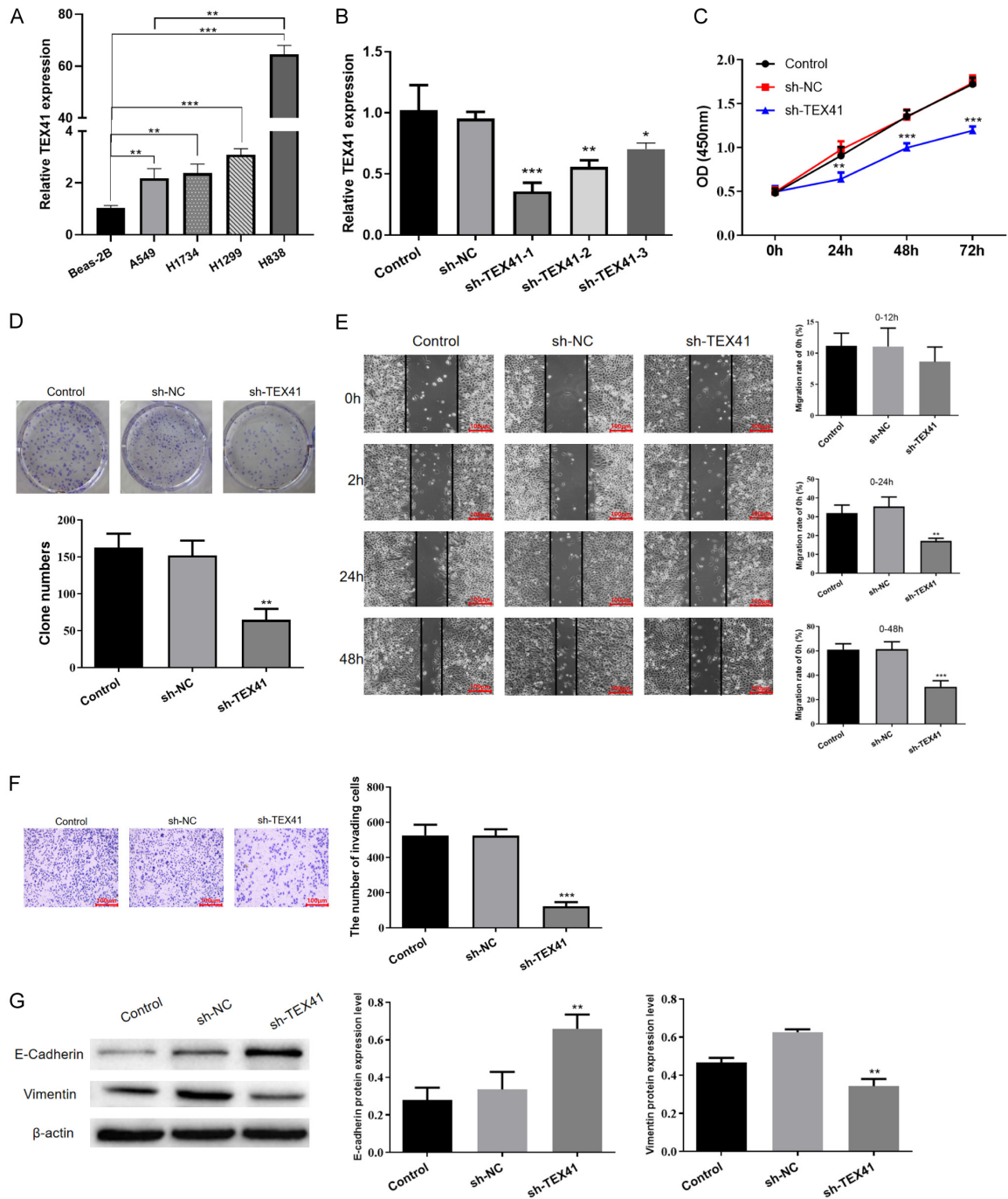
Figure 3. Silencing TEX41 inhibited the malignant biological behavior of lung adenocarcinoma (LUAD) cells. A. TEX41 levels in LUAD cells. B. Qualitative polymerase chain reaction (qPCR) detection of TEX41 levels in LUAD cells introduced with small hairpin RNA (shRNA) targeting TEX41 (sh-TEX41) or negative control (sh-NC). C. Disrupting TEX41 inhibited H838 cell proliferation measured by the Cell Counting Kit-8 assay. D. TEX41 knockdown inhibited H838 cell proliferation by the colony-forming assay. E. TEX41 knockdown suppressed H838 cell migration. F. The Transwell assay indicated that TEX41 interference suppressed H838 cell invasion. G. E-cadherin and vimentin protein levels after TEX41 knockdown. *$P<0.05$, **$P<0.01$, ***$P<0.001$ vs. negative control (NC).

upregulated Runx2 expression and increased LC3II/I protein levels, although no significant changes were observed in p62 and Beclin-1 expression levels ([Figure S2I](#)). Collectively, our

*in vivo* studies suggest that TEX41 can promote LUAD BM, which is probably associated with increased Runx2 and autophagy protein levels.
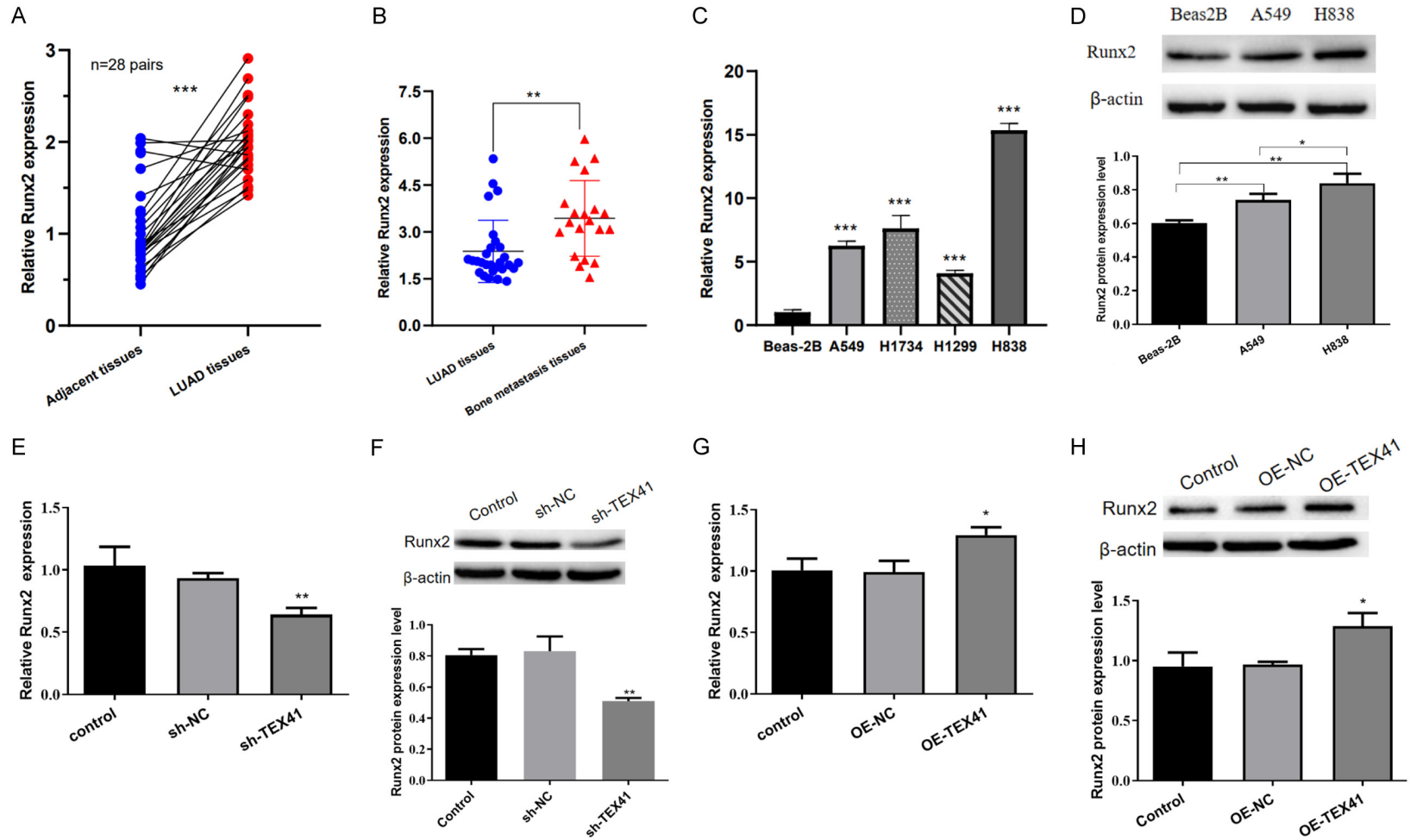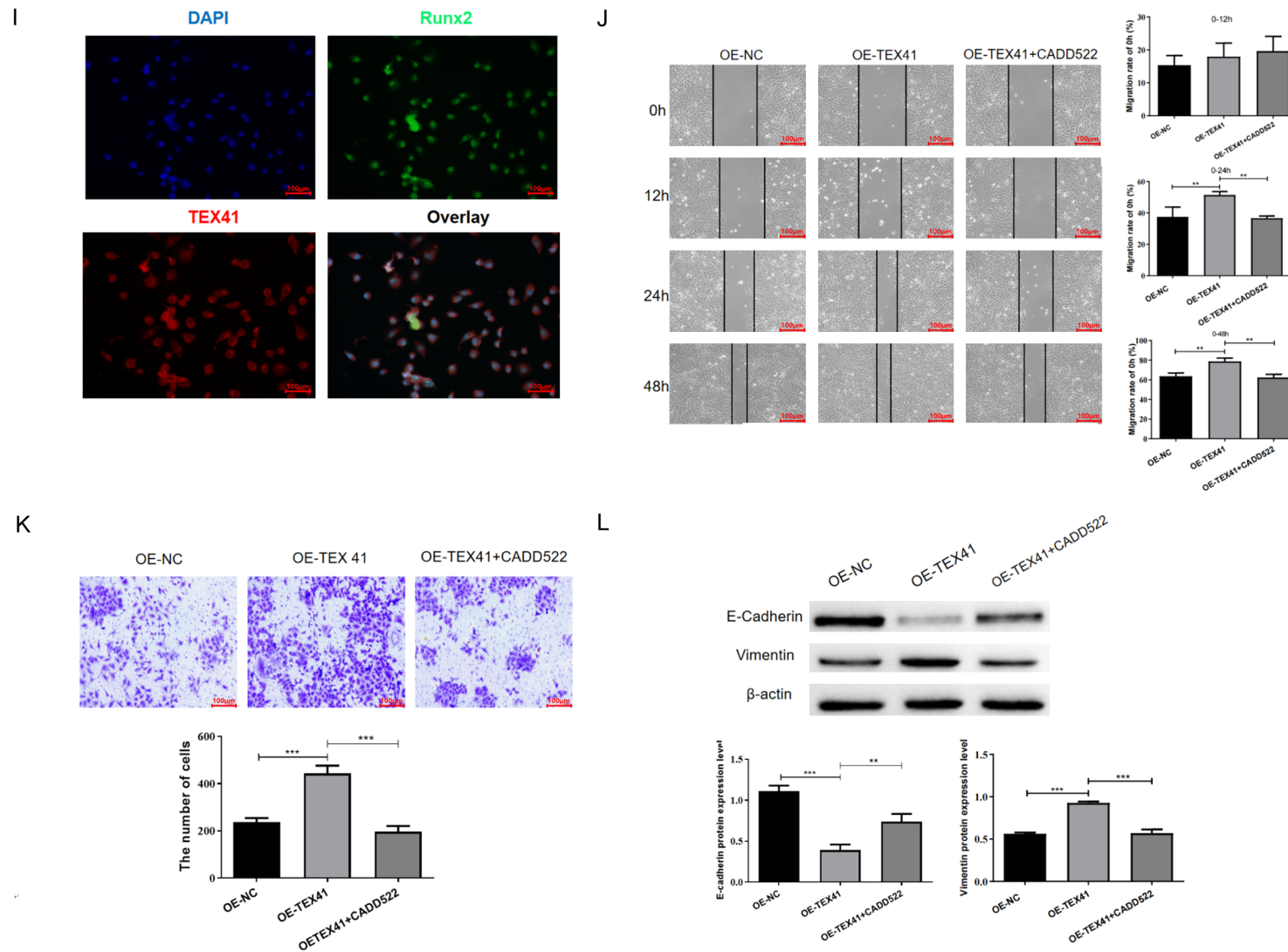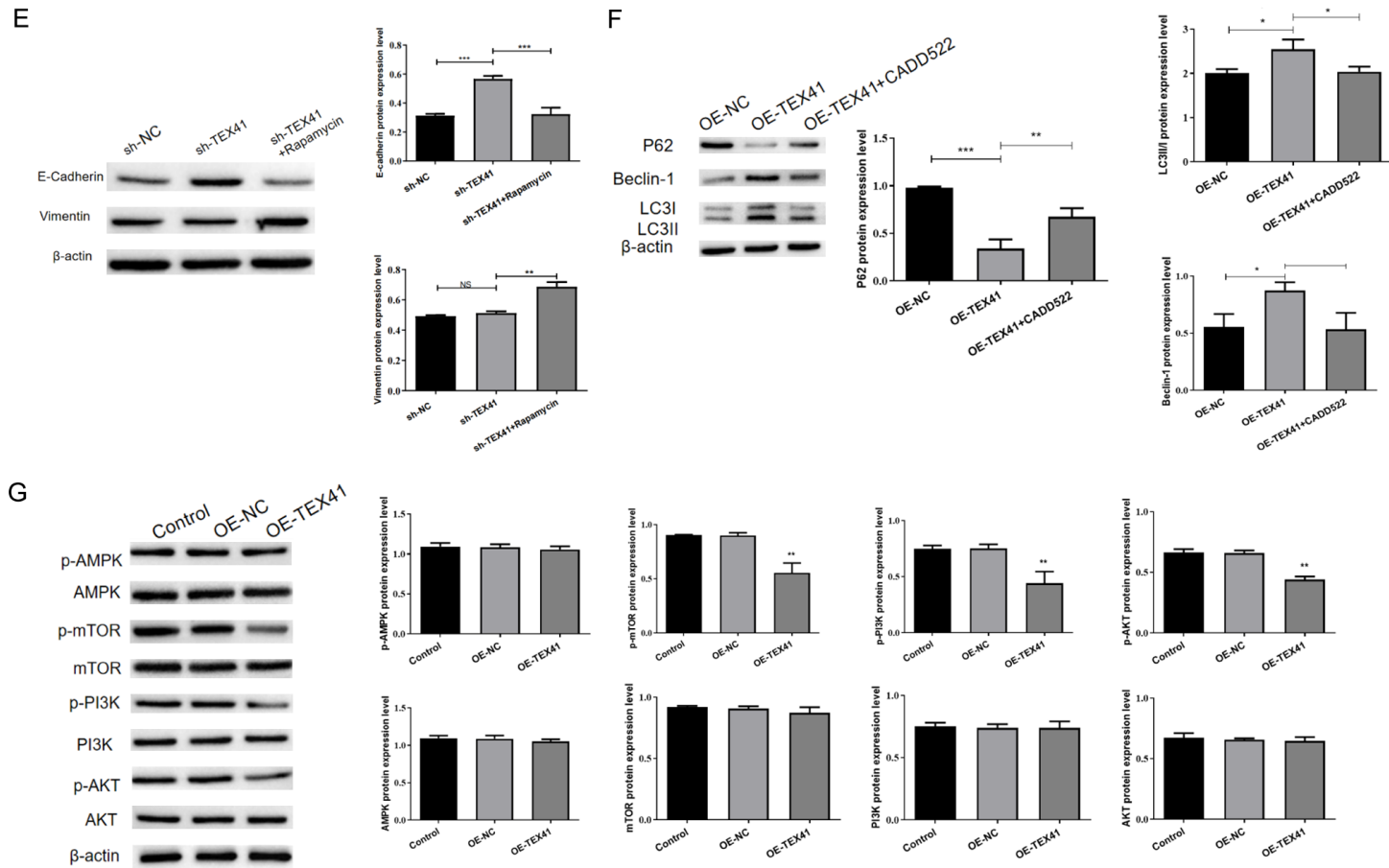
Figure 4. TEX41 affected lung adenocarcinoma (LUAD) cell migration, invasion and metastasis via Runx2. A. Runx2 expression in primary LUAD. B. Runx2 expression in LUAD bone metastasis (BM). C, D. Runx2 was highly expressed in LUAD cell lines. E, F. TEX41 interference inhibited Runx2 mRNA and protein expressions. G, H. TEX41 overexpression upregulated Runx2 mRNA and protein expressions. I. Fluorescence in-situ hybridization showed that TEX41 and Runx2 colocalized in the nucleus. J-L. TEX41 affected LUAD cell migration, invasion and metastasis via Runx2. *$P<0.05$, **$P<0.01$, ***$P<0.001$.
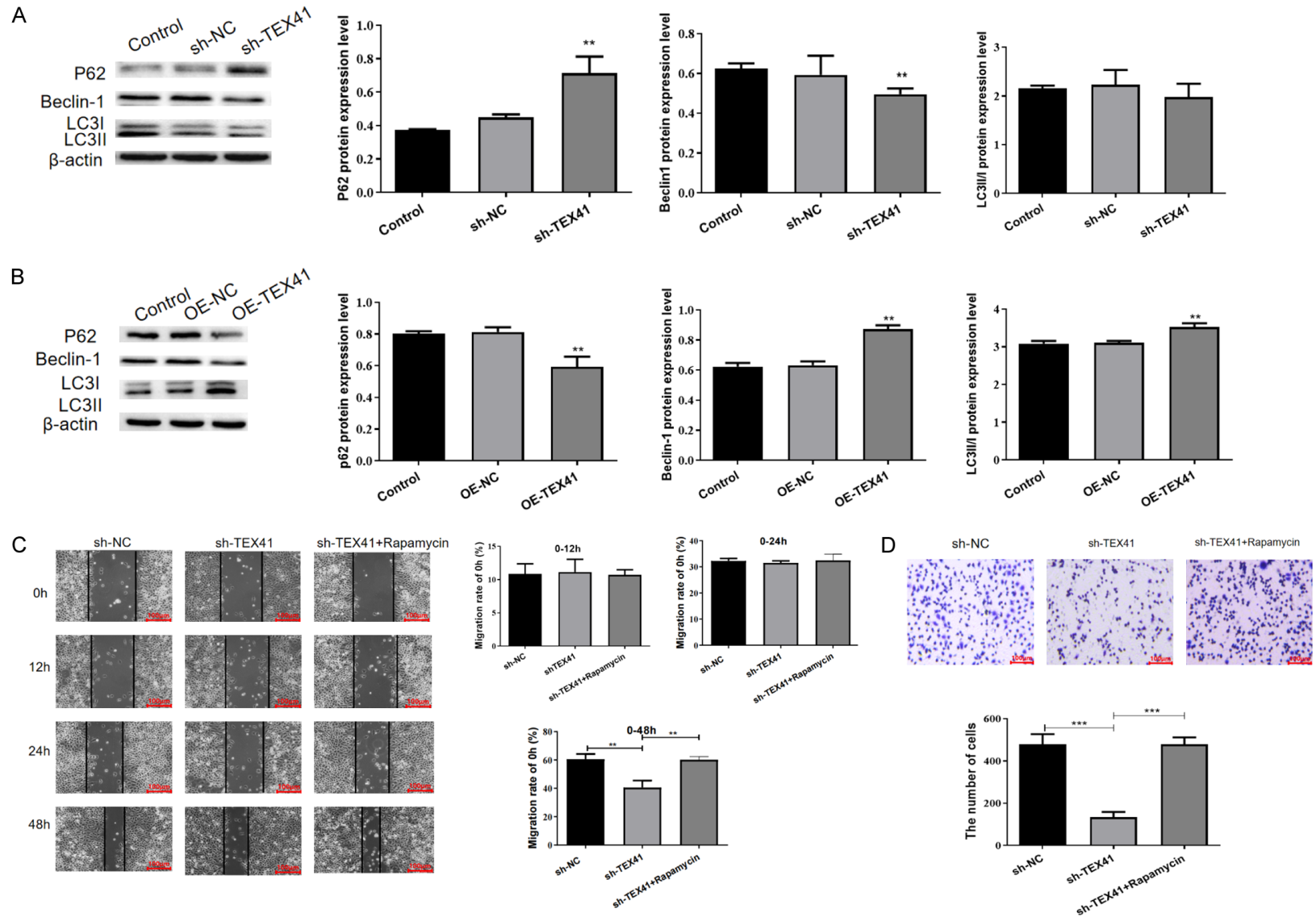
Figure 5. TEX41 regulated lung adenocarcinoma (LUAD) cell migration, invasion and metastasis by mediating autophagy. A. TEX41 interference altered autophagy-related protein levels. B. TEX41 overexpression altered autophagy-related protein levels. C. TEX41 enhanced LUAD cell migration through autophagy. D. TEX41 affected LUAD cell invasiveness via autophagy. E. TEX41 promoted LUAD cell metastasis through autophagy. F. TEX41 affected LUAD cell autophagy via Runx2. G. TEX41 regulated autophagy via the phosphoinositide 3-kinase (PI3K)/AKT axis. *$P<0.05$, **$P<0.01$, ***$P<0.001$.
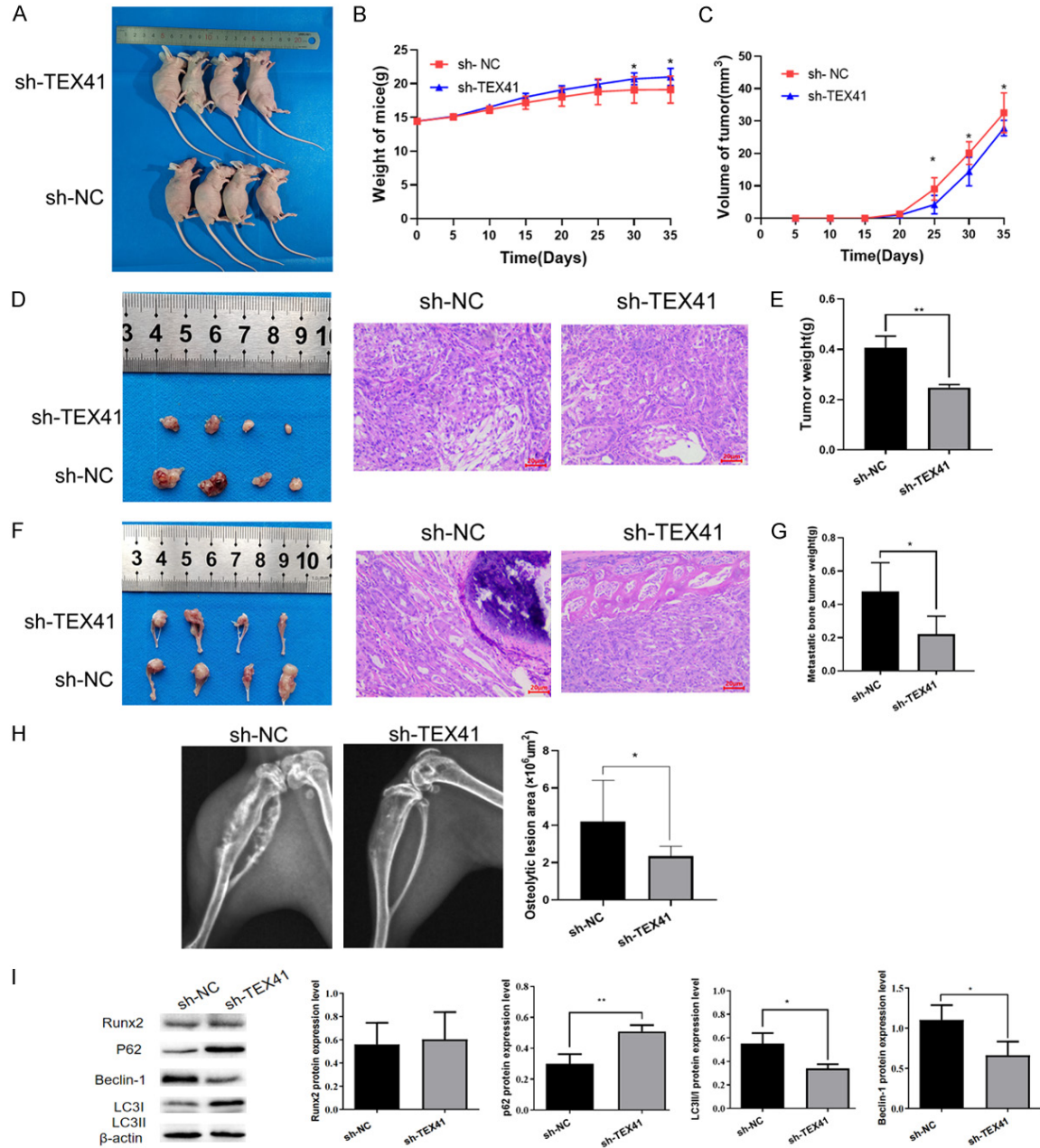
Figure 6. TEX41 interference inhibited the formation of subcutaneous lung adenocarcinoma (LUAD) and bone metastasis (BM) in nude mice treated with small hairpin RNA (shRNA) targeting negative control (sh-NC, n=4) or TEX41 (sh-TEX41, n=4). A. Large specimens of nude mice. B. Body weight. C. Subcutaneous tumor volume growth curves. D. Subcutaneous tumor sections from nude mice and representative HE staining images of tissues from the two groups. E. Subcutaneous tumors weight. F. BM sections from nude mice and representative HE staining images of tissues from the two groups. G. BM tumors weight. H. BM areas measured by X-ray. I. Runx2 and autophagy marker protein levels in BM from nude mice were determined by immunoblotting. *P<0.05, **P<0.01, ***P<0.001.

Discussion

With the rapid development of gene chips and next-generation sequencing, an increasing number of lncRNAs have been identified and studied, including TEX41. Our previous findings

have indicated that TEX41 is increased in LUAD BM tissue and is closely related to the BM signaling pathway [29]. BM is a prominent factor contributing to the poor prognosis of malignant tumors, and characterizing BM pathogenesis to uncover effective therapeutic targets remains

a clinical challenge. Studies have shown that the lncRNAs MAYA [30], PCAT6 [31], SOX2OT [32], NEAT1 [33] and SNHG3 [34] are associated with BM development in malignant tumors. LncRNAs could be adopted as early diagnostic markers, efficacy and prognosis predictors, and early detection markers for LUAD BM. Our results suggest that high TEX41 expression can predict deeper lymph node invasion and more advanced clinical stage and correlates with the prognosis of LUAD patients with BM, which has potential clinical value.

By examining the putative biological functions of TEX41 *in vitro*, we found that TEX41 could promote the growth, migration, invasion and metastasis of LUAD cells. Moreover, TEX41 promoted subcutaneous tumor formation and BM in nude mice, indicating that TEX41 plays a pro-BM role in adapting LUAD cells to grow in the bone microenvironment. TEX41 can promote the malignant biological behavior of melanoma cells by targeting the miR-103a-3p-C1QB axis [35]. TEX41 can also promote leukemia cell growth *in vitro* [36]. To further clarify the specific mechanism through which TEX41 exerts carcinogenic effects in LUAD, we used bioinformatics to predict the transcription factors that TEX41 might act on. One of the top 30 predicted transcription factors was Runx2, which we correlated with the BM signaling pathway in LUAD in our previous study [29]. Hence, we speculated that TEX41 might modulate LUAD BM via Runx2.

Runx2 is a bone-specific transcription factor involved in BM and associated with many BM-related factors [37]. Runx2 is closely linked to breast cancer cell adaption to the bone microenvironment and BM enhancement [38]. Runx2 affects the formation of BM in prostate cancer under the regulation of miR-466 [39]. In addition to a potential role in BM, Runx2 may also be involved in the onset of EMT, leading to distant metastasis [40]. In the current study, we found that TEX41 overexpression promoted migration, invasion and metastasis of LUAD cells, and the effects could be effectively reversed by Runx2 inhibitor CADD522. Furthermore, FISH revealed that TEX41 and Runx2 are colocalized in the nucleus, indicating that Runx2 could be a target for TEX41.

Currently, most studies assume that autophagy plays a role in cancer promotion in advanced tumors [41, 42]. MiR-106a enhances the migration, invasion and EMT of LUAD cells, leading to BM through a mechanism that partly depends on autophagy [43]. Regulating autophagy is expected to become a breakthrough in treating BM [44]. Runx2 is known to interact with the autophagy pathway [45], and evidence suggests that Runx2 can promote cancer via the PI3K-AKT axis [46]. In addition, a study on the mechanism of autophagy in osteogenic differentiation showed that Runx2 expression was elevated in osteogenic differentiation, which was mainly associated with the activation of cellular autophagy regulated by the AMPK pathway [47]. Therefore, Runx2 might represent a key autophagy regulator, possibly through PI3K-AKT or AMPK signaling.

In the current study, we revealed that TEX41 target gene functions were mainly enriched in cancer-related PI3K-AKT and autophagy signaling pathways. Consequently, we speculate that TEX41 mediates LUAD cell migration, invasion and metastasis by regulating Runx2 expression and affecting autophagy. Our results suggest that the TEX41-Runx2 signaling axis regulates autophagy in LUAD cells and that the oncogenic effects of TEX41 partially depend on autophagy. Furthermore, TEX41 can partially regulate autophagy via the PI3K-AKT axis. Our *in vivo* tumor experiments also suggest that TEX41 could significantly promote BM formation, and the expressions of Runx2 and autophagy marker proteins in BM further indicate that the effects of TEX41 on LUAD BM are related to Runx2 and autophagy. However, there are limitations in this study. Whether TEX41 and Runx2 interact through a direct binding site requires further investigation, and the specific regulatory mechanism between TEX41 and Runx2 needs to be elucidated.

In conclusion, our study identified TEX41 as a possible biomarker for the prognosis of LUAD BM. TEX41 could promote the migration, invasion and BM of LUAD cells by regulating Runx2 and autophagy through the PI3K-AKT signaling pathway (**Figure 7**). Our study provides a new theoretical basis for finding effective targets for treating LUAD BM.

Acknowledgements
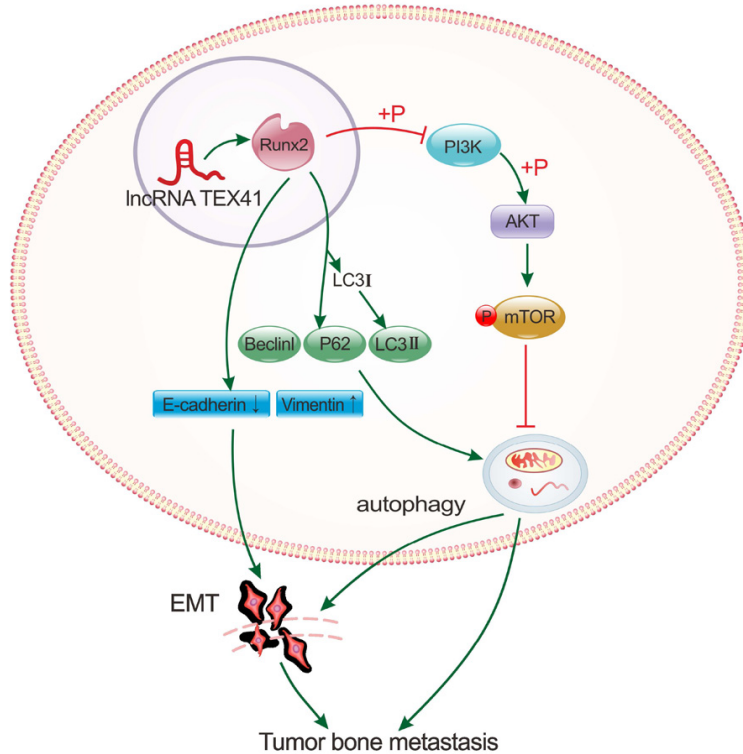
Figure 7. Schematic illustration of the possible mechanism through which the long noncoding RNA (lncRNA) TEX41 mediates lung adenocarcinoma (LUAD) bone metastasis (BM). TEX41 regulates Runx2 expression in the nucleus, altering autophagy-related protein expression. By promoting autophagy through the phosphoinositide 3-kinase (PI3K)/AKT axis, TEX41 facilitates epithelial-mesenchymal transition (EMT), mediating LUAD migration, invasion and BM.

Disclosure of conflict of interest

None.

Address correspondence to: Lin Xie, Department of Gastrointestinal Oncology, The Third Affiliated Hospital of Kunming Medical University, Yunnan Cancer Hospital, Yunnan Cancer Center, Kunming, Yunnan, China. E-mail: xielinyanghan@163.com

References

[1] Sung H, Ferlay J, Siegel RL, Laversanne M, Soerjomataram I, Jemal A and Bray F. Global cancer statistics 2020: GLOBOCAN estimates of incidence and mortality worldwide for 36 cancers in 185 countries. CA Cancer J Clin 2021; 71: 209-49.

[2] Cao M and Chen W. Epidemiology of lung cancer in China. Thorac Cancer 2019; 10: 3-7.

[3] Li Y, Shi J, Yu S, Wang L, Liu J, Ren J, Gao S, Hui Z, Li J, Wu N, Yang B, Liu S, Qin M, Wang D, Liao X, Xing X, Du L, Yang L, Liu Y, Zhang Y, Zhang K, Qiao Y, He J, Dai M and Yao H; Health Economic Evaluation Working Group CSPiUC. Effect of socioeconomic status on stage at diagnosis of lung cancer in a hospital-based multicenter retrospective clinical epidemiological study in China, 2005-2014. Cancer Med 2017; 6: 2440-2452.

[4] Huang Q, Wei H, Wu Z, Li L, Yao L, Sun Z, Li L, Lin Z, Xu W, Han S, Cao W, Xu Y, Song D, Yang X and Xiao J. Preferentially expressed antigen of melanoma prevents lung cancer metastasis. PLoS One 2016; 11: e0149640.

[5] Niu Y, Lin Y, Pang H, Shen W, Liu L and Zhang H. Risk factors for bone metastasis in patients with primary lung cancer: a systematic review. Medicine (Baltimore) 2019; 98: e14084.

[6] Coleman RE, Croucher PI, Padhani AR, Clézardin P, Chow E, Fallon M, Guise T, Colangeli S, Capanna R and Costa L. Bone metastases. Nat Rev Dis Primers 2020; 6: 83.

[7] Beermann J, Piccoli MT, Viereck J and Thum T. Non-coding RNAs in development and disease: background, mechanisms, and therapeutic approaches. Physiol Rev 2016; 96: 1297-325.

[8] Yao RW, Wang Y and Chen LL. Cellular functions of long noncoding RNAs. Nat Cell Biol 2019; 21: 542-51.

[9] Huarte M. The emerging role of lncRNAs in cancer. Nat Med 2015; 21: 1253-61.

[10] Liu SJ, Dang HX, Lim DA, Feng FY and Maher CA. Long noncoding RNAs in cancer metastasis. Nat Rev Cancer 2021; 21: 446-460.

[11] Schmitt AM and Chang HY. Long noncoding RNAs in cancer pathways. Cancer Cell 2016; 29: 452-463.

[12] Ji P, Diederichs S, Wang W, Böing S, Metzger R, Schneider PM, Tidow N, Brandt B, Buerger H, Bulk E, Thomas M, Berdel WE, Serve H and Müller-Tidow C. MALAT-1, a novel noncoding RNA, and thymosin beta4 predict metastasis

and survival in early-stage non-small cell lung cancer. Oncogene 2003; 22: 8031-41.

[13] Wang R, Shi Y, Chen L, Jiang Y, Mao C, Yan B, Liu S, Shan B, Tao Y and Wang X. The ratio of FoxA1 to FoxA2 in lung adenocarcinoma is regulated by LncRNA HOTAIR and chromatin remodeling factor LSH. Sci Rep 2015; 5: 17826.

[14] Qiu M, Xu Y, Yang X, Wang J, Hu J, Xu L and Yin R. CCAT2 is a lung adenocarcinoma-specific long non-coding RNA and promotes invasion of non-small cell lung cancer. Tumour Biol 2014; 35: 5375-80.

[15] Jiang X, Yuan Y, Tang L, Wang J, Zhang D and Duan L. Systematic analysis and validation of the prognosis, immunological role and biology function of the ferroptosis-related lncRNA GSEC/miRNA-101-3p/CISD1 axis in lung adenocarcinoma. Front Mol Biosci 2022; 8: 793732.

[16] Wu Q and Jiang J. LncRNA MAFG-AS1 promotes lung adenocarcinoma cell migration and invasion by targeting miR-3196 and regulating SOX12 expression. Mol Biotechnol 2022; 64: 970-983.

[17] Ding DX, Li Q, Shi K, Li H, Guo Q and Zhang YQ. LncRNA NEAT1-miR-101-3p/miR-335-5p/miR-374a-3p/miR-628-5p-TRIM6 axis identified as the prognostic biomarker for lung adenocarcinoma via bioinformatics and meta-analysis. Transl Cancer Res 2021; 10: 4870-4883.

[18] Tang X, Hua X, Peng X, Pei Y and Chen Z. Integrated dissection of lncRNA-miRNA-mRNA pairs and potential regulatory role of lncRNA PCAT19 in lung adenocarcinoma. Front Genet 2022; 12: 765275.

[19] Wang X, Zheng S, Yang F, Zhang W, Zhao D, Xue X, Lin Q, He Y, Hu G and Hu Y. lncRNA HITT inhibits metastasis by attenuating Rab5-mediated endocytosis in lung adenocarcinoma. Mol Ther 2022; 30: 1071-1088.

[20] Liang XH, Jackson S, Seaman M, Brown K, Kempkes B, Hibshoosh H and Levine B. Induction of autophagy and inhibition of tumorigenesis by beclin 1. Nature 1999; 402: 672-6.

[21] Levy JMM, Towers CG and Thorburn A. Targeting autophagy in cancer. Nat Rev Cancer 2017; 17: 528-542.

[22] Iachettini S, Trisciuoglio D, Rotili D, Lucidi A, Salvati E, Zizza P, Di Leo L, Del Bufalo D, Ciriolo MR, Leonetti C, Steegborn C, Mai A, Rizzo A and Biroccio A. Pharmacological activation of SIRT6 triggers lethal autophagy in human cancer cells. Cell Death Dis 2018; 9: 996.

[23] Kimmelman AC and White E. Autophagy and tumor metabolism. Cell Metab 2017; 25: 1037-1043.

[24] Chen H, Hu Z, Sang M, Ni S, Lin Y, Wu C, Mu Y, Liu K, Wu S, Li N and Xu G. Identification of an autophagy-related lncRNA prognostic signa-

ture and related tumor immunity research in lung adenocarcinoma. Front Genet 2021; 12: 767694.

[25] Deng Y, Zhang F, Sun ZG and Wang S. Development and validation of a prognostic signature associated with tumor microenvironment based on autophagy-related lncRNA analysis in hepatocellular carcinoma. Front Med (Lausanne) 2021; 8: 762570.

[26] Liang L, Huan L, Wang J, Wu Y, Huang S and He X. LncRNA RP11-295G20.2 regulates hepatocellular carcinoma cell growth and autophagy by targeting PTEN to lysosomal degradation. Cell Discov 2021; 7: 118.

[27] Song Y, Du J, Lu P, Zou Q, Zeng S, Liu M, Hu X, Ma W, Lin H, Liu X and Niu F. LncRNA NFYC-AS1 promotes the development of lung adenocarcinomas through autophagy, apoptosis, and MET/c-Myc oncogenic proteins. Ann Transl Med 2021; 9: 1621.

[28] Wang Y, Li Z, Xu S, Li W, Chen M, Jiang M and Fan X. LncRNA FIRRE functions as a tumor promoter by interaction with PTBP1 to stabilize BECN1 mRNA and facilitate autophagy. Cell Death Dis 2022; 13: 98.

[29] Han L, Yao Z, Xie L, Li D, Wang C, Yang Y, Yang J, Huang Z, Li K, Zhang Y, Ye L, Tan Z, Liu Y, Chen Q, Wang T and Yang Z. Transcriptome Sequencing reveals the expressed profiles of mRNA and ncRNAs and regulate network via ceRNA mediated molecular mechanism of lung adenocarcinoma bone metastasis in Xuanwei. Transl Cancer Res 2021; 10: 73-87.

[30] Li C, Wang S, Xing Z, Lin A, Liang K, Song J, Hu Q, Yao J, Chen Z, Park PK, Hawke DH, Zhou J, Zhou Y, Zhang S, Liang H, Hung MC, Gallick GE, Han L, Lin C and Yang L. A ROR1-HER3-lncRNA signalling axis modulates the Hippo-YAP pathway to regulate bone metastasis. Nat Cell Biol 2017; 19: 106-119.

[31] Lang C, Yin C, Lin K, Li Y, Yang Q, Wu Z, Du H, Ren D, Dai Y and Peng X. m6 A modification of lncRNA PCAT6 promotes bone metastasis in prostate cancer through IGF2BP2-mediated IGF1R mRNA stabilization. Clin Transl Med 2021; 11: e426.

[32] Ni J, Zhang X, Li J, Zheng Z, Zhang J, Zhao W and Liu L. Tumour-derived exosomal lncRNA-SOX2OT promotes bone metastasis of non-small cell lung cancer by targeting the miRNA-194-5p/RAC1 signalling axis in osteoclasts. Cell Death Dis 2021; 12: 662.

[33] Mo C, Huang B, Zhuang J, Jiang S, Guo S and Mao X. LncRNA nuclear-enriched abundant transcript 1 shuttled by prostate cancer cells-secreted exosomes initiates osteoblastic phenotypes in the bone metastatic microenvironment via miR-205-5p/runt-related transcription factor 2/splicing factor proline-and gluta-

mine-rich/polypyrimidine tract-binding protein 2 axis. Clin Transl Med 2021; 11: e493.

[34] Sun Z, Hu J, Ren W, Fang Y, Hu K, Yu H, Liao D, Liu S, Zhou L, He T and Zhang Y. LncRNA SNHG3 regulates the BMSC osteogenic differentiation in bone metastasis of breast cancer by modulating the miR-1273g-3p/BMP3 axis. Biochem Biophys Res Commun 2021; 594: 117-123.

[35] Zheng Y, Zhou W, Li M, Xu R, Zhang S, Liu Y and Cen Y. IRF4-activated TEX41 promotes the malignant behaviors of melanoma cells by targeting miR-103a-3p/C1QB axis. BMC Cancer 2021; 21: 1339.

[36] Orlandella FM, Smaldone G, Salvatore G, Vitagliano L, Cianflone A, Parasole R, Beneduce G, Menna G, Salvatore M and Mirabelli P. The lncRNA TEX41 is upregulated in pediatric B-cells acute lymphoblastic leukemia and it is necessary for leukemic cell growth. Biomark Res 2021; 9: 54.

[37] Pratap J, Lian JB, Javed A, Barnes GL, van Wijnen AJ, Stein JL and Stein GS. Regulatory roles of Runx2 in metastatic tumor and cancer cell interactions with bone. Cancer Metastasis Rev 2006; 25: 589-600.

[38] Vishal M, Swetha R, Thejaswini G, Arumugam B and Selvamurugan N. Role of Runx2 in breast cancer-mediated bone metastasis. Int J Biol Macromol 2017; 99: 608-614.

[39] Colden M, Dar AA, Saini S, Dahiya PV, Shahryari V, Yamamura S, Tanaka Y, Stein G, Dahiya R and Majid S. MicroRNA-466 inhibits tumor growth and bone metastasis in prostate cancer by direct regulation of osteogenic transcription factor RUNX2. Cell Death Dis 2017; 8: e2572.

[40] Tan CC, Li GX, Tan LD, Du X, Li XQ, He R, Wang QS and Feng YM. Breast cancer cells obtain an osteomimetic feature via epithelial-mesenchymal transition that have undergone BMP2/RUNX2 signaling pathway induction. Oncotarget 2016; 7: 79688-79705.

[41] Ganzleben I, Neurath MF and Becker C. Autophagy in cancer therapy-molecular mechanisms and current clinical advances. Cancers (Basel) 2021; 13: 5575.

[42] Amaravadi RK, Kimmelman AC and Debnath J. Targeting autophagy in cancer: recent advances and future directions. Cancer Discov 2019; 9: 1167-1181.

[43] Han L, Huang Z, Liu Y, Ye L, Li D, Yao Z, Wang C, Zhang Y, Yang H, Tan Z, Tang J and Yang Z. MicroRNA-106a regulates autophagy-related cell death and EMT by targeting TP53INP1 in lung cancer with bone metastasis. Cell Death Dis 2021; 12: 1037.

[44] Wang Y, Wu N and Jiang N. Autophagy provides a conceptual therapeutic framework for bone metastasis from prostate cancer. Cell Death Dis 2021; 12: 909.

[45] Tandon M, Othman AH, Ashok V, Stein GS and Pratap J. The role of Runx2 in facilitating autophagy in metastatic breast cancer cells. J Cell Physiol 2018; 233: 559-571.

[46] Tandon M, Chen Z and Pratap J. Runx2 activates PI3K/Akt signaling via mTORC2 regulation in invasive breast cancer cells. Breast Cancer Res 2014; 16: R16.

[47] Yang Y, Lin Z, Cheng J, Ding S, Mao WW, Shi S, Liang B and Jiang L. The roles of autophagy in osteogenic differentiation in rat ligamentum fibroblasts: evidence and possible implications. FASEB J 2020; 34: 8876-8886.

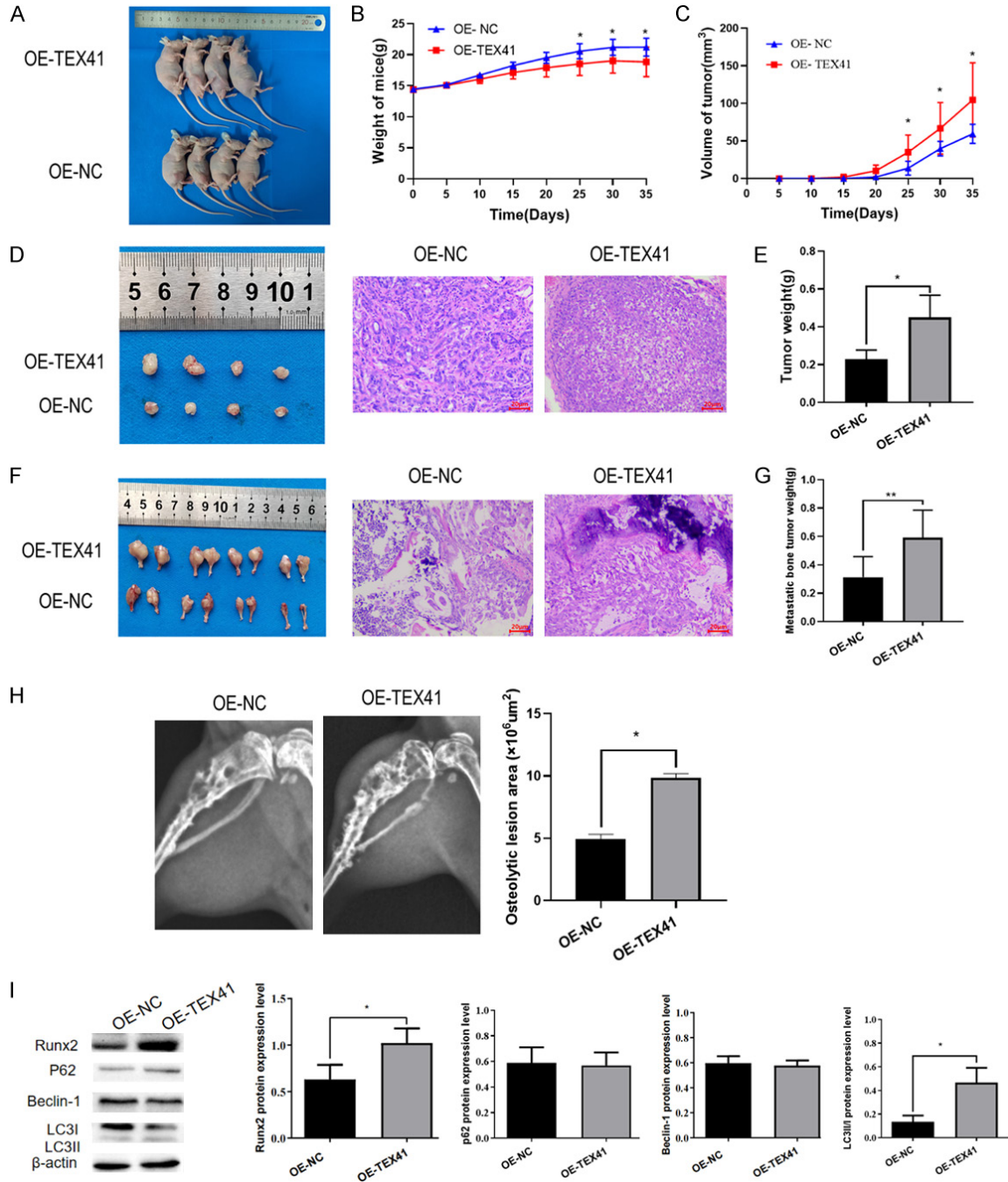## Overexpression of TEX41 promoted malignant biological behavior of LUAD cells

In contrast to the results of the TEX41 interference assay, the results of the cell function assay showed that overexpression of TEX41 promoted the growth, proliferation, migration, and invasion of LUAD A549 cells (Figure S1B-E). Overexpression of TEX41 could downregulate E-cadherin expression and upregulate vimetin expression (Figure S1F), indicating that overexpression of TEX41 enhanced the metastatic ability of LUAD cells.
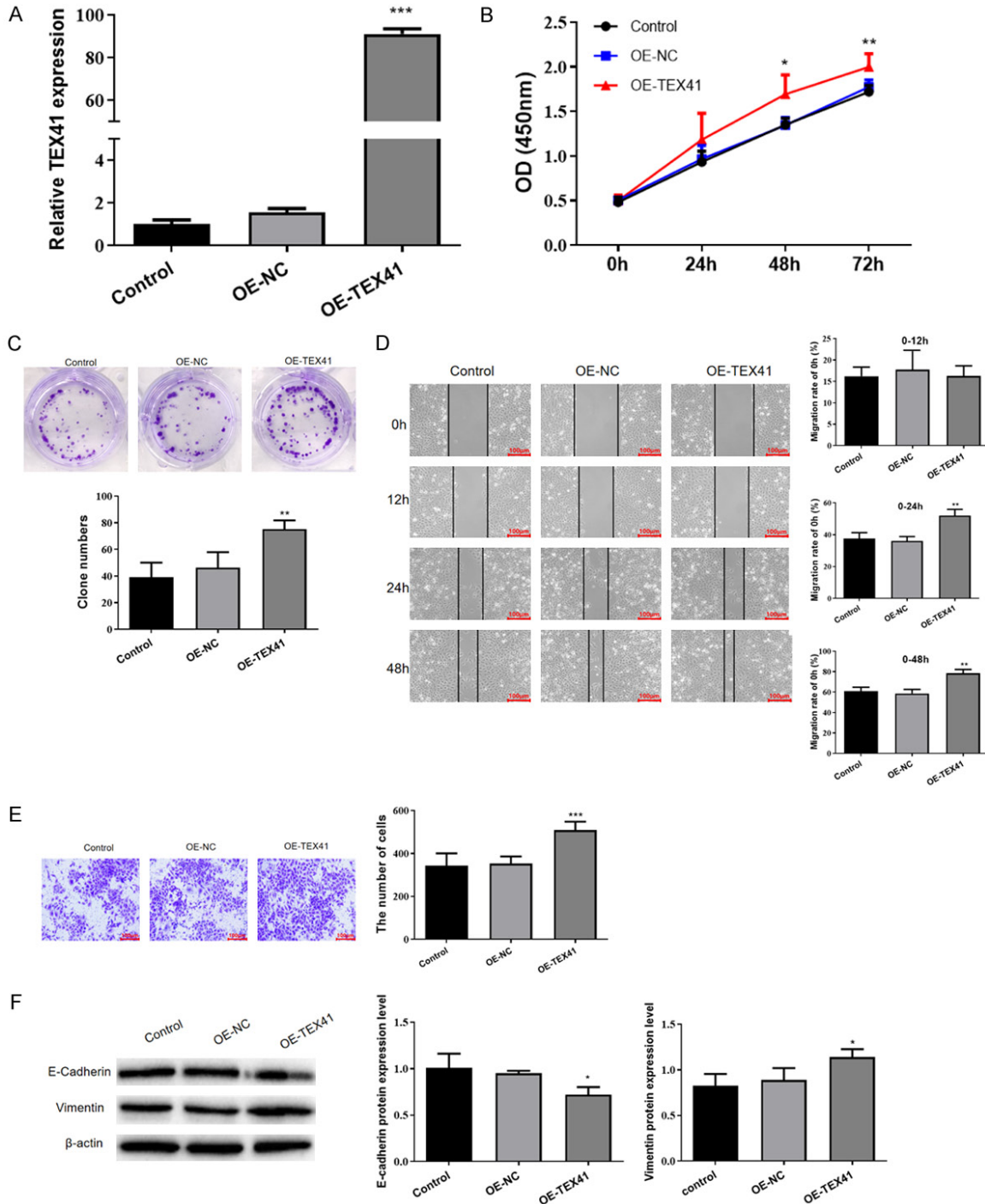
Figure S1. Overexpression of TEX41 promoted malignant biological behavior of lung adenocarcinoma (LUAD) cell. A. The expression of TEX41 in LUAD cell line introduced with OE-TEX41 or OE-NC was analyzed by qualitative polymerase chain reaction (qPCR). B. Cell Counting Kit-8 (CCK-8) assay suggested that overexpression of TEX41 promote proliferation of A549 cells. C. Overexpression of TEX41 promoted the independent proliferative ability of A549 cells by colony formation assays. D. Scratch assay showed that overexpression of TEX41 promoted the migration of A549 cells. E. Transwell assays were performed to indicate that overexpression of TEX41 promotes invasion of A549 cells. F. The levels of E-cadherin and vimetin protein after overexpression of TEX41 were determined by western blot. *P<0.05, **P <0.01, ***P<0.001 vs. negative control (NC).

TEX41 promoted the formation of subcutaneous tumors and bone metastasis of LUAD in nude mice

Figure S2. Overexpression of TEX41 promoted the formation of subcutaneous tumors and bone metastasis of lung adenocarcinoma (LUAD) in nude mice. A. Large specimens of nude mice. B. Body weight growth curve in nude mice. C. Subcutaneous tumor volume growth curve in nude mice. D. Hematoxylin and eosin (HE) staining of subcutaneous tumor sections from nude mice. E. Subcutaneous tumors weight. F. HE staining of BM sections from nude mice. G. BM tumors weight. H. BM areas measured by X-ray. I. Runx2 and autophagy marker protein levels in BM from nude mice were determined by immunoblotting. *P<0.05, **P<0.01, ***P<0.001.